HAL
open science

Enantioselectivity of human AMP, dTMP and UMP-CMP kinases

Julie A. C. Alexandre, Béatrice Roy, Dimitri Topalis, Sylvie S. Pochet, Christian Périgaud, Dominique Deville-Bonne

To cite this version:

Julie A. C. Alexandre, Béatrice Roy, Dimitri Topalis, Sylvie S. Pochet, Christian Périgaud, et al.. Enantioselectivity of human AMP, dTMP and UMP-CMP kinases. Nucleic Acids Research, 2007, pp.1-10. 10.1093/nar/gkm479 . pasteur-00166118

HAL Id: pasteur-00166118

https://pasteur.hal.science/pasteur-00166118

Submitted on 1 Jun 2022

HAL is a multi-disciplinary open access archive for the deposit and dissemination of scientific research documents, whether they are published or not. The documents may come from teaching and research institutions in France or abroad, or from public or private research centers.

L'archive ouverte pluridisciplinaire **HAL**, est destinée au dépôt et à la diffusion de documents scientifiques de niveau recherche, publiés ou non, émanant des établissements d'enseignement et de recherche français ou étrangers, des laboratoires publics ou privés.

Distributed under a Creative Commons Attribution - NonCommercial 4.0 International License

Published online 10 July 2007 Nucleic Acids Research, 2007, Vol. 35, No. 14 4895–4904
doi:10.1093/nar/gkm479

Enantioselectivity of human AMP, dTMP and UMP-CMP kinases

Julie A.C. Alexandre[1], Béatrice Roy[2], Dimitri Topalis[1], Sylvie Pochet[3], Christian Périgaud[2] and Dominique Deville-Bonne[1,*]

[1]Laboratoire d'Enzymologie Moléculaire, FRE 2852-CNRS-Université Paris 6, 4, place Jussieu, 75005 Paris [2]Institut des Biomolécules Max Mousseron (IBMM), UMR 5247 CNRS-Universités Montpellier 1 et 2, case courrier 1705, Bâtiment Chimie 17, Université Montpellier 2, Place Eugène Bataillon, 34095 Montpellier cedex 5 and [3]Unité de Chimie Organique, URA CNRS 2128, Institut Pasteur, 28 rue du Dr Roux, 75724 Paris Cedex15, France

Received April 27, 2007; Revised May 30, 2007; Accepted May 31, 2007

ABSTRACT

L-Nucleoside analogues such as lamivudine are active for treating viral infections. Like D-nucleosides, the biological activity of the L-enantiomers requires their stepwise phosphorylation by cellular or viral kinases to give the triphosphate. The enantioselectivity of NMP kinases has not been thoroughly studied, unlike that of deoxyribonucleoside kinases. We have therefore investigated the capacity of L-enantiomers of some natural (d)NMP to act as substrates for the recombinant forms of human uridylate-cytidylate kinase, thymidylate kinase and adenylate kinases 1 and 2. Both cytosolic and mitochondrial adenylate kinases were strictly enantioselective, as they phosphorylated only D-(d)AMP. L-dTMP was a substrate for thymidylate kinase, but with an efficiency 150-fold less than D-dTMP. Both L-dUMP and L-(d)CMP were phosphorylated by UMP-CMP kinase although much less efficiently than their natural counterparts. The stereopreference was conserved with the 2′-azido derivatives of dUMP and dUMP while, unexpectedly, the 2′-azido-D-dCMP was a 4-fold better substrate for UMP-CMP kinase than was CMP. Docking simulations showed that the small differences in the binding of D-(d)NMP to their respective kinases could account for the differences in interactions of the L-isomers with the enzymes. This *in vitro* information was then used to develop the *in vivo* activation pathway for L-dT.

INTRODUCTION

Recent developments indicate that L-nucleosides and L-nucleoside analogues are potent anti-viral, anti-tumour and even anti-malarial agents (1–4). The L-derivative, lamivudine (β-L-2′,3′-dideoxy-3′-thiacytidine, 3TC), has been approved for treating both HIV and HBV, while emtricitabine (β-L-2′,3′-dideoxy-5-fluoro-3′-thiacytidine, FTC) is used in HIV therapy. Telbivudine (β-L-thymidine, L-dT) was recently approved for treating hepatitis B by the US Food and Drug Administration. Many L-nucleosides are currently in advanced clinical trials for the treatment of a variety of virus diseases. These include clevudine [1-(2-fluoro-5-methyl-β-L-arabinofuranosyl)uracil, L-FMAU], elvucitabine (2′,3′-didehydro-2′,3′-dideoxy-β-L-5-fluorocytidine, β-L-d4FC), valtorcitabine (val-β-L-2′-deoxycytidine, val-L-dC), pentacept (2′,3′-didehydro-2′,3′-dideoxy-3′-fluoro-β-L-cytidine, β-L-3′-Fd4C) and β-L-2′-Fd4C (2′,3′-didehydro-2′,3′-dideoxy-2′-fluoro-β-L-cytidine). Most L-enantiomers considered for treating virus diseases have similar activities to their D-counterparts, but are less sensitive to degrading enzymes and have better safety profiles (5,6). These properties are due mainly to the enantioselectivity of the enzymes that interact with these substrates *in vivo* (7). L-nucleosides must be phosphorylated by cellular or viral kinases before they can reach the targeted virus enzymes. The enantioselectivity of the enzymes involved in nucleoside *de novo* synthesis and salvage pathway is governed by no general rule. Each individual metabolic enzyme must therefore be studied. Among the four deoxyribonucleoside kinases in human cells, cytosolic thymidine kinase 1 (TK1) is strictly enantioselective while mitochondrial thymidine kinase 2 (TK2) is less specific (8–10). Deoxycytidine kinase

*To whom correspondence should be addressed. Tel: +33 1 44 27 59 93, Fax: +33 1 44 27 59 94; Email: ddeville@ccr.jussieu.fr

The authors wish it to be known that, in their opinion, the first two authors should be regarded as joint First Authors.

© 2007 The Author(s)
This is an Open Access article distributed under the terms of the Creative Commons Attribution Non-Commercial License (http://creativecommons.org/licenses/by-nc/2.0/uk/) which permits unrestricted non-commercial use, distribution, and reproduction in any medium, provided the original work is properly cited.

Downloaded from https://academic.oup.com/nar/article/35/14/4895/1014948 by Bibliothèque Universitaire de médecine - Nîmes user on 01 June 2022

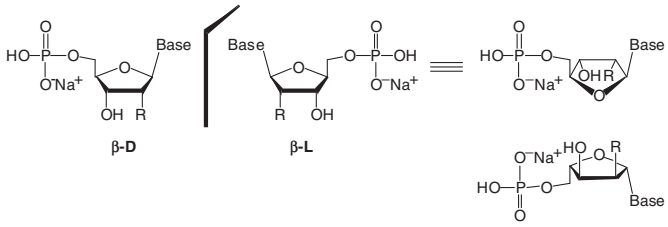

L-NMP	Compound	Base	R
L-AMP	β-L-adenosine 5′-monophosphate	adenine	OH
L-dAMP	β-L-2′-deoxyadenosine 5′-monophosphate	adenine	H
L-dUMP	β-L-2′-deoxyuridine 5′-monophosphate	uracile	H
N_3-L-dUMP	β-L-2′-azido-2′-deoxyuridine 5′-monophosphate	uracile	N_3
L-CMP	β-L-cytidine 5′-monophosphate	cytosine	OH
L-dCMP	β-L-2′-deoxycytidine 5′-monophosphate	cytosine	H
N_3-L-dCMP	β-L-2′-azido-2′-deoxycytidine 5′-monophosphate	cytosine	N_3
L-dTMP	β-L-2′-deoxythymidine 5′-monophosphate	thymine	H

Figure 1. Structures of β-L and β-D (deoxy)ribonucleoside monophosphates (Base = adenine, thymine, uracil, cytosine).

(dCK) and deoxyguanosine kinase (dGK) are poorly enantioselective *in vitro* (9,11–12). The phosphorylation of nucleoside monophosphates and their analogues to their diphosphate derivatives is then carried out by NMP kinases in both *de novo* and salvage pathways. The NMP kinases in human cells include one dTMP kinase, one UMP-CMP kinase, six isoenzymes of adenylate kinase and several guanylate kinases (13). Only the abilities of hUMP-CMP and dTMP kinases to phosphorylate some L-deoxynucleoside monophosphate analogues has been studied to date (14–15). Finally, NDPK is strictly enantioselective (16). The final step can be carried out by phosphoglycerate kinase, which has a broad substrate specificity (17–18). Other ATP-synthesizing enzymes such as creatine kinase can also be involved in this step (19). Triphosphorylated L-derivatives can interact with viral polymerases, acting as competitive inhibitors or alternate substrates, usually leading to chain termination. Viral polymerases incorporate L-derivatives more readily than do the human ones (20–21). Nucleoside degrading enzymes, such as nucleoside deaminases and phosphorylases, tend to be strictly selective for D-nucleotides although only limited data is available (11,22). The lack of degradation of L-nucleosides has however been demonstrated in mice, where L-nucleosides were gradually excreted in the unchanged form following intraperitoneal administration (5). 5′-Nucleotidases also seem to be moderately to highly enantioselective (7,23). The ribonucleotide reductases, which catalyze the *de novo* conversion of ribonucleotides to 2′-deoxyribonucleotides, are also key enzymes in DNA replication and repair. *In vitro*, these enzymes are inhibited by 2′-azido-2′-deoxynucleoside 5′-diphosphates (24–27). However, N_3-D-dUrd is not cytotoxic due to its poor intracellular phosphorylation. The mechanism of enzyme inactivation and the enzymatic monophosphorylation of the parent nucleosides has been thoroughly studied (24–25). More recently, we have shown that ribonucleotide reductase is enantiospecific with respect to the natural configuration of the sugar moiety (26–27). This report examines the phosphorylation of the β-D and β-L stereoisomers of 2′-azido pyrimidine monophosphates by human UCK, TMPK and AKs and characterizes the enantioselectivity and the possible cross-activities of these three human kinases for natural (d)NMP (Figure 1).

Part of this work was presented during the XVIIth Round Table for Nucleosides, Nucleotides and Nucleic Acids in Bern, in September 2006.

MATERIALS AND METHODS

Natural D-nucleotides were purchased from Sigma chemicals (St Louis, MO, USA). MABA-dTDP was synthesized as described (28).

Synthesis of L-nucleoside 5′-monophosphates

L-dA, L-dU, L-dC and L-dT were a generous gift from Idenix Pharmaceuticals (http://www.idenix.com). L-ribonucleosides were synthesized starting from L-ribose following usual procedures. The azidonucleosides were synthesized as previously described (26). L-Nucleoside 5′-monophosphates (L-NMP) were prepared by selective 5′-phosphorylation of the corresponding L-nucleosides with $POCl_3$ in triethylphosphate (29). L-NMPs were purified on DEAE-Sephadex A-25 (elution: linear gradient of TEAB pH 7.6 from 10 to 300 mM) followed by RP18 chromatography (elution: water to methanol 50%). The triethylammonium counter ions were exchanged for sodium by passing the nucleotide solution through a DOWEX-AG 50WX2-400 column. Yields were 43–80%. The structures and purities of L-NMP were assessed by nuclear magnetic resonance (^{1}H, ^{13}C, ^{31}P), fast-atom-bombardment MS, UV spectroscopy, HPLC and polarimetry. In some cases, it was necessary to separate the nucleoside 5′-monophosphate from traces of nucleoside 3′-monophosphate. This was done by semi-preparative HPLC using Hypercarb®, a porous graphite carbon stationary phase (30).

The physico-chemical properties of the 2′-azido-2′-deoxy D-nucleotides were identical, except for the $[\alpha]_D^{20}$ value, to those of the corresponding 2′-azido-2′-deoxy L-nucleotides.

N_3-L-dUMP: $[\alpha]_D^{20}$ + 29 (c 1.1, MeOH); ^{1}H NMR (D_2O, 300 MHz) δ 7.96 (δ, 1H, J = 8.1 Hz, H–6), 5.93 (d, 1H, J = 5.3 Hz, H–1′), 5.87 (d, 1H, J = 8.1 Hz, H5), 4.48 (pt, 1H, J = 5.1 Hz, H3′), 4.30 (pt, 1H, J = 5.4 Hz, H2′), 4.16 (sl, 1H, H4′), 4.04–3.90 (m, 2H, H5′, H5″); ^{13}C NMR (D_2O, 300 MHz) δ 166.2, 151.6, 141.6, 102.7, 86.9, 84.4, 70.3, 65.4, 63.2; ^{31}P NMR (D_2O, 300 MHz) δ + 2.47; UV (H_2O) λ_{max} 260 nm (ε 9400); MS FAB + m/z 372 $(M + H)^+$, 350 $(M - Na + 2H)^+$. N_3-D-dUMP: $[\alpha]_D^{20}$ − 29 (c 1.1, MeOH). N_3-L-dCMP: $[\alpha]_D^{20}$ − 18 (c 1, H_2O); ^{1}H NMR (D_2O, 300 MHz) δ 8.07 (d, 1H, J = 7.6 Hz, H–6), 6.14 (d, 1H, J = 7.6 Hz, H5), 6.06 (d, 1H, J = 4.5 Hz, H–1′), 4.54 (pt, 1H, J = 5.4 Hz, H3′), 4.34 (pt, 1H, J = 5.1 Hz, H2′), 4.26–4.22 (m, 1H, H4′), 4.16–4.04 (m, 2H, H5′, H5″); ^{13}C NMR (D_2O, 300 MHz) δ 166.1, 157.3, 141.3, 96.6, 87.7, 83.5, 69.8, 66.0, 62.9;

Downloaded from https://academic.oup.com/nar/article/35/14/4895/1014948 by Bibliothèque Universitaire de médecine - Nîmes user on 01 June 2022

^{31}P NMR (D_2O, 300 MHz) $\delta + 2.15$; UV (H_2O) λ_{max} 269 nm (ε 10 500); MS FAB + m/z 371 $(M + H)^+$, 349 $(M - Na + 2H)^+$. N_3-D-dCMP: $[\alpha]_D^{20} + 18$ (c 1.1, H_2O).

Bacterial production and purification of His-tagged NMP kinases

Human UCK, TMPK, AK1 and AK2 were produced in *Escherichia coli* as recombinant proteins as previously reported (15,31, Topalis, personal communication). *E. coli* Rosetta (DE3)pLysS cells transformed with the appropriate expression plasmid were grown at 37°C in LB medium supplemented with 34 $\mu g \cdot ml^{-1}$ chloramphenicol and 50 $\mu g \cdot ml^{-1}$ kanamycin. Gene expression was induced by adding 0.5 mM IPTG when the absorbance at 600 nm reached 0.8, and cells were grown at 30°C for a further 3 h. The cells were harvested, lysed by sonication and centrifuged at 5000 r.p.m., 8°C, for 30 min. The supernatant was loaded onto a Ni-NTA column (Qiagen, Germany) equilibrated with lysis buffer (50 mM Tris-HCl, 300 mM NaCl, 10 mM imidazole, pH = 8.0). The column was washed with lysis buffer and the proteins eluted with a linear gradient of imidazole, (0–250 mM). The fractions containing the enzyme were pooled and dialysed against dialysis buffer (50 mM Tris-HCl pH = 7.4, 20 mM NaCl, 1 mM DTT, 50% glycerol). SDS-PAGE indicated that the protein was over 95% pure.

Enzymatic assays

The activities of the NMP kinases were followed by a coupled spectrophotometric assay (32). Assays were carried out at 37°C in the following reaction mixture (total volume: 140 µl): 50 mM Tris-HCl, pH = 7.4, 50 mM KCl, 5 mM $MgCl_2$, 1 mM ATP, 0.2 mM NADH, 1 mM phosphoenolpyruvate, 1 mM DTT, 4 $U \cdot \mu l^{-1}$ pyruvate kinase, 4 $U \cdot \mu l^{-1}$ lactate dehydrogenase. As the NDP kinase from *Dictyostelium discoideum* is strictly enantioselective, this enzyme was only added (4 $U \cdot \mu l^{-1}$) for assays with a D-enantiomer substrate (32). The reaction was started by adding the (d)NMP or (d)NMP analogue and the decrease in absorbance at 340 nm was measured. The kinase concentrations were 4 nM to 8 µM in order to measure initial rates below 0.2 ΔA/min. For inhibition studies, the inhibitor was added after the enzyme, the reaction was then started by adding the substrate(s). The results were analysed using the KALEIDAGRAPH software. Assays were carried out in duplicate or triplicate.

Only 0.2 mM ATP was added in the reaction mixture for studies on the inhibition of hAK1 and hAK2. Inhibition was studied at three inhibitor concentrations: 0, 400 and 600 µM L-AMP for inhibiting the phosphorylation of D-AMP by hAK1, and 0, 38 and 134 µM L-AMP for inhibiting the phosphorylation of D-dAMP by hAK2. The inhibitor was added immediately after the enzyme, and adding the substrate started the reaction. Data were plotted on double reciprocal plots and the K_I values were determined by plotting the slopes against the concentrations of inhibitor.

Fluorescence assays

The dissociation constants of hTMPK for both dTMP enantiomers were measured using a fluorescence assay (28). Briefly, the binding of the fluorescent probe MABA-dTDP to hTMPK in buffer T (50 mM Tris-HCl, pH = 7.5, 5 mM $MgCl_2$, 50 mM KCl and 5% glycerol) resulted in a 190% increase in fluorescence intensity (excitation at 340 nm and emission at 430 nm with emission and excitation slits at 2 and 4 nm, respectively). The binding constant was determined by titration of the fluorophore with the enzyme ($K_D = 6\,\mu M$). Competition titrations with D- or L-d(T/U)MP were done by mixing MABA-dTDP (6 µM) with the enzyme (6 µM), so that, as recommended, about half of the fluorophore was enzyme-bound at the start of the experiment (33). Upon addition of increasing amounts of ligand, the fluorescence probe was gradually displaced from the enzyme active site and the resulting decreases in fluorescence were monitored. The total specific signal was determined at the end of each experiment by adding excess dTDP. The data were corrected for dilution and plotted: IC_{50} values were obtained at half-displacement. The IC_{50} values are related to the dissociation constants for the ligand, K_D, and for the fluorophore MABA-dTDP, K_D^F, by the following equation (33):

$$K_D = IC_{50} K_D^F B / \left[AP + B\left(P - A + B - K_D^F\right) \right] \quad (1)$$

where B is the initial concentration of bound MABA-TDP, A is the total concentration of MABA-dTDP and P is the total concentration of kinase (considered to be monomers).

Modelling studies

L-nucleotides and nucleotides analogues were drawn on Molsoft (http://www.molsoft.com, 2D to 3D converter) and Smiles Translator (http://cactus.nci.nih.gov/services/translate/) to produce the PDB files. The conformation of the sugar ring was checked by visualizing the molecules within the PyMOL graphic system and, if necessary, modified to the β-L or β-D configuration, as desired (34). Docking of the L-nucleotides and nucleotide analogues was performed using ArgusLab software (35). The binding site was defined from the coordinates of the ligand in the original PDB files 2UKD for hUCK and 1E2D for hTMPK. Docking precision was set to 'high' and the 'flexible ligand docking' mode was used for each docking run. Resulting complexes were visualized with the PyMOL graphic system and the diagrams for each nucleotide analogue/NMP kinase model obtained were drawn using Chemdraw CambridgeSoft (ChemDraw, CambridgeSoft Corporation, USA, http://www.camsoft.com).

RESULTS AND DISCUSSION

Strict stereospecificity of recombinant human AMP kinases 1 and 2

The activities of the major adenylate kinases hAK1 (cytosolic) and hAK2 (in the inter-membrane space of mitochondria) were measured *in vitro* as a function of the

Downloaded from https://academic.oup.com/nar/article/35/14/4895/1014948 by Bibliothèque Universitaire de médecine - Nîmes user on 01 June 2022

Table 1. Catalytic parameters for the (d)AMP enantiomers with human AMP kinases 1 and 2

Enzyme	Substrate	K_M (mM)	Relative V_{max} (%)	k_{cat}/K_M ($M^{-1}s^{-1}$)
hAK1	D-AMP	0.14 ± 0.02	100[a]	3×10^6 (100[b])
	D-dAMP	1.5 ± 0.3	48 ± 4	1.6×10^5 (5.3)
	D-CMP	3.0 ± 0.8	5.6	9.5×10^3 (0.32)
	D-dCMP	–[c]	–[c]	–[c]
	D-UMP	6 ± 2	2.9	2.6×10^3 (0.08)
	D-dUMP	–[c]	–[c]	–[c]
	L-AMP	–[c]	–[c]	–[c]
	L-dAMP	–[c]	–[c]	–[c]
hAK2	D-AMP[d]	0.08 ± 0.02	16	10^6 (33)
	D-dAMP	0.21 ± 0.05	22	5×10^5 (17)
	D-CMP	6 ± 1	13	10^4 (0.33)
	D-dCMP	–[c]	–[c]	–[c]
	D-UMP	9 ± 2	0.32	180 (0.006)
	D-dUMP	–[c]	–[c]	–[c]
	L-AMP	–[c]	–[c]	–[c]
	L-dAMP	–[c]	–[c]	70 (0.002)

[a]The relative V_{max} were obtained by comparing the k_{cat} value of the substrates to that of D-AMP. For V_{max} standardization, 100 corresponds to 1240 µmol of substrate transformed/min/mg, i.e. to a $k_{cat} = 500\,s^{-1}$.
[b]The relative efficiencies were obtained by comparing the k_{cat}/K_M ($M^{-1}s^{-1}$) value of a substrate to that of D-AMP.
[c]Non detectable.
[d]hAK2 activity was inhibited by [AMP] > 0.3 mM, ($K_I = 0.5$ mM).

D- and L-(d)AMP concentrations as well as of pyrimidine nucleoside monophosphates. Human AK1 and AK2 were both specific for the D-enantiomers. They did not phosphorylate L-(d)NMP, except for hAK2 having very little action on L-dAMP corresponding to a 'catalytic efficiency' about 10^4 smaller than for the D-stereoisomer (Table 1). The rate of D-(d)AMP phosphorylation increased with the substrate concentration, as expected for Michaelis curves. The maximum rate V_{max} of D-AMP phosphorylation by hAK2 was not reached due to substrate inhibition at concentrations above 0.3 mM (data not shown). This inhibition is generally attributed to unproductive binding of the ligand at the same site or at a secondary site. The reaction rates for hAK2 were slightly below those for hAK1 but were almost compensated for by the K_M values, resulting in somewhat similar catalytic efficiencies as might be expected from the similarities of their active site sequences. D-dAMP was a slightly poorer substrate than D-AMP for both hAK1 and hAK2. The deoxyribonucleotides, D-dCMP and D-dUMP, were not substrates for the AKs although these enzymes phosphorylated the pyrimidine nucleotides, D-CMP and D-UMP, to a minor extent (Table 1) (15).

L-AMP was bound by both enzymes. It competitively inhibited the phosphorylation of D-AMP and D-dAMP by hAK1 and hAK2, with an estimated K_I of 200 µM for hAK1 and 18 µM for hAK2 (data not shown). D-dAMP was used because the mitochondrial AK2 was inhibited by excess D-AMP. The binding of L-nucleotides to the AMP site of hAK1 and hAK2 was thus unproductive. Additionally, L-(d)AMP was also not a substrate for hUCK or hTMPK (data not shown).

Table 2. Catalytic parameters for the dTMP and dUMP enantiomers with human TMP kinase

Substrate	K_M (mM)	k_{cat} (s^{-1})	k_{cat}/K_M ($M^{-1}s^{-1}$)	K_I (mM)
D-dTMP	0.020 ± 0.005	3.0 ± 0.1	1.5×10^5 (100[a])	–
D-dUMP	0.17 ± 0.01	4.8 ± 0.6	2.8×10^4 (18)	2.6 ± 0.9
L-dTMP	0.38 ± 0.07	0.34 ± 0.03	900 (0.7)	5 ± 1
L-dUMP	2.3 ± 0.2	0.13 ± 0.01	60 (0.04)	–

[a]Relative efficiency expressed by comparing the k_{cat}/K_M ($M^{-1}s^{-1}$) value for a substrate to that of dTMP.

Despite this poor phosphorylation, L-dA reduced the virus load *in vivo* in the woodchuck model of chronic B hepatitis although less efficiently than L-dC or L-dT (6). The other isoenzymes of AK, i.e. hAK3, 4, 5 and 6 could contribute to the phosphorylation of L-(d)AMP and explain this *in vivo* activity (36–37).

Relaxed stereospecificity of recombinant human dTMP kinase

The recent approval of L-dT for treating hepatitis B has prompted us to study the phosphorylation of L-dTMP by hTMPK. The catalytic efficiency of the enzyme for L-dTMP was around 0.7% that D-dTMP (Table 2). The catalytic turnover number k_{cat} was 10 times smaller than that for D-dTMP, while the K_M was 20-fold higher, resulting in a lower k_{cat}/K_M (about $900\,M^{-1}s^{-1}$) (Figure 2A, Table 2). L-dTMP also gave rise to substrate inhibition at 1 mM and the K_I value was estimated to be 5 mM (Table 2). D-dUMP was a good substrate with an efficiency in the $10^4\,M^{-1}s^{-1}$ range, as already reported (38), but the phosphorylation of L-dUMP very slow ($k_{cat}/K_M = 60\,M^{-1}s^{-1}$).

The relative binding constants for the L- and D-isomers of dTMP were measured using the fluorescent competition assay based on the fluorescent probe MABA-dTDP (28). The dissociation constants for D-dTMP and L-dTMP from hTMPK were 2 µM and 45 µM, respectively (Figure 2B). The K_D ratio was 22, comparable to the K_M ratio, i.e. 19 (Table 2). Using the same assay, the nucleosides, D- and L-dT, also competed with MABA-dTDP and had K_D values of 40 and 450 µM, respectively, indicating that the L-nucleoside also binds to the active site less efficiently than its D-counterpart. The affinity of the enzyme for L-dTMP ($K_D = 45$ µM), was greater than its affinity for D-dUMP ($K_D = 150$ µM), which is a good substrate of the enzyme (Figure 2B).

Activity of recombinant human UMP-CMP kinase with D- and L-nucleoside monophosphates

L-dUMP and L-dCMP were substrates of hUCK, but they were phosphorylated much more slowly than were the natural nucleotides, despite the K_M of the enzyme being slightly more favourable for the L-compounds. The K_M values were 1.3 mM for D-dUMP and 1.0 mM for D-dCMP, compared to 0.70 mM for L-dUMP and 0.73 mM for L-dCMP (Figure 3, Table 3). But the reaction rate was 20 times slower for L-dUMP than for D-dUMP and 100 times slower for L-dCMP than for

Downloaded from https://academic.oup.com/nar/article/35/14/4895/1014948 by Bibliothèque Universitaire de médecine - Nîmes user on 01 June 2022

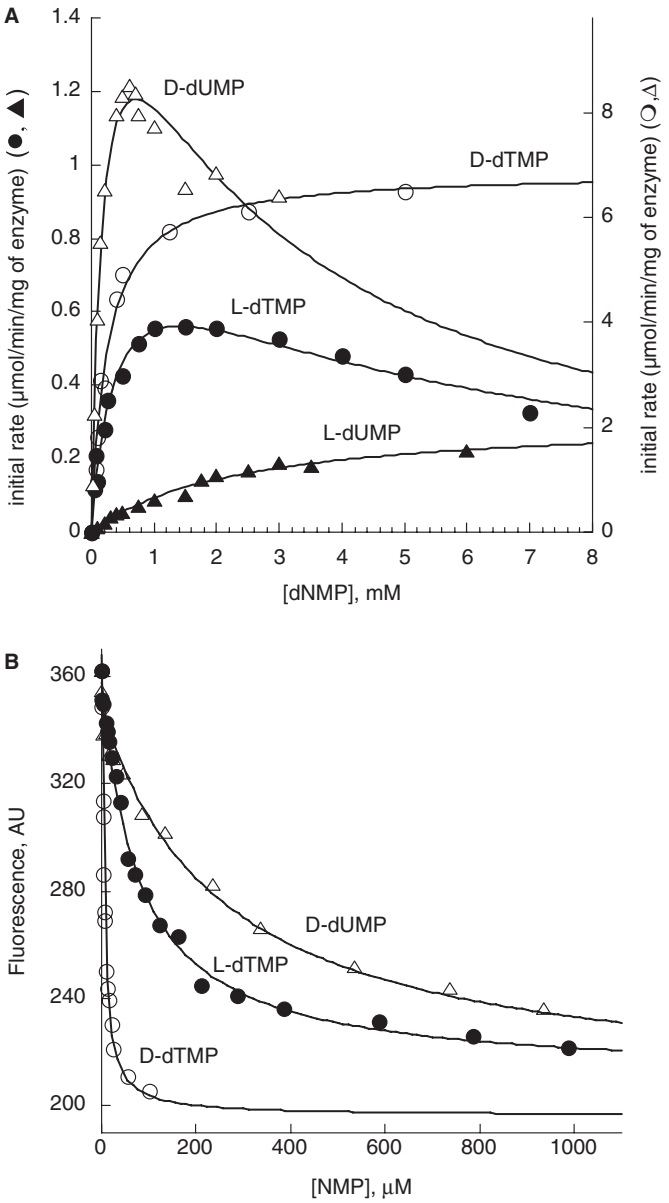

Figure 2. Reaction of human dTMP kinase with the natural nucleoside monophosphates dTMP and dUMP and their corresponding L-enantiomers. (**A**) Saturation curves of dTMP kinase with (open circle) D-dTMP, (filled circle) L-dTMP, (open triangle) D-dUMP and (filled triangle) L-dUMP. The experiments were carried out in the presence of 2 mM ATP and 2 mM Mg^{2+} using the standard coupled assay. The quantity of enzyme used in each experiment was: 0.18 µM for D-dTMP; 3 µM for L-dTMP; 0.12 µM for D-dUMP and 5 µM for L-dUMP. The K_M and k_{cat} values obtained by fitting to a hyperbole are shown in Table 1. The reaction rates v for D-dUMP and L-dTMP as substrates [S] were best fitted with Equation (2). $v = (V \bullet [S])/(K_M + [S] + ([S]^2/K_I))$ (2) (**B**) Fluorescence competition assays of different substrates with MABA-dTDP bound to human dTMP kinase. The fluorescence of MABA-dTDP (6 µM) was monitored at 430 nm (excitation wavelength at 340 nm, excitation slit = 2 nm, emission slit = 4 nm) in the presence of 6 µM enzyme in T buffer resulting in the binding of 40% of the fluorophore. The complex was titrated with (open circle) D-dTMP, (filled circle) L-dTMP and (open triangle) D-dUMP. The IC_{50} values were 4.6, 82 and 260 µM respectively. The dissociation constants K_D calculated according to Equation (1) were 2 µM, 45 µM and 0.15 mM, respectively.

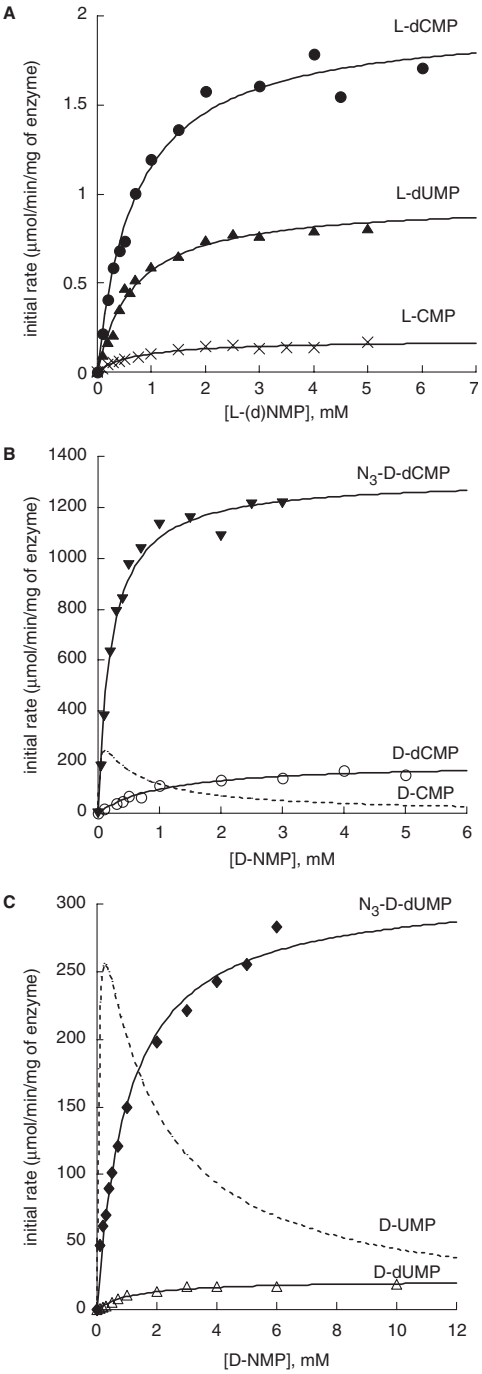

Figure 3. Reaction of human UMP-CMP kinase with the enantiomers of (d)CMP and (d)UMP and their 2′-azido-derivatives. (**A**) Saturation curves of hUMP-CMP kinase as a function L-derivatives as substrates: (filled circle) L-dCMP, (filled triangle) L-dUMP and (cross mark) L-CMP obtained with respectively 0.4, 1 and 7.6 µM of hUCK in the reaction mixture. (**B**) Saturation curves of hUMP-CMP kinase with the D-enantiomers of (open circle) dCMP and (inverted triangle) N_3-D-dCMP. The quantity of enzyme used was 4 nM for dCMP and 0.8 nM for N_3-D-dCMP. The dash line represents the saturation curve with D-CMP obtained with 4 nM hUCK as shown in (15) and fitted to Equation (2). (**C**) Saturation curves of hUMP-CMP kinase with the D-enantiomers of (open triangle) dUMP and (filled diamond) N_3-D-dUMP. The quantity of enzyme used was 4 nM for dUMP and N_3-D-dUMP. The dash line represents the saturation curve with D-UMP obtained with 4 nM hUCK as shown in (15) and fitted to Equation (2).

Downloaded from https://academic.oup.com/nar/article/35/14/4895/1014948 by Bibliothèque Universitaire de médecine - Nîmes user on 01 June 2022

its D-counterpart. L-CMP was also phosphorylated by hUCK but it was a very poor substrate for this enzyme, with a catalytic efficiency of $100\,M^{-1}\,s^{-1}$, 10 times lower than that for L-dCMP and 10^4 times lower than for D-CMP. This decreased efficiency is due to a much lower k_{cat}, as the K_M was similar to that for L-dCMP (0.75 mM). Excess of L-CMP was inhibitory, unlike the natural substrate. The L-derivate that was the best substrate for hUCK was L-dCMP, but it was far less efficient than the monophosphate form of the antiviral analogue L-3TC. L-3TCMP is indeed phosphorylated to L-3TCDP by hUCK with a catalytic efficiency k_{cat}/K_M of $2.8 \times 10^5\,M^{-1}\,s^{-1}$ (15).

Activity of recombinant human UMP-CMP kinase with 2′-azido-2′-deoxynucleotides

The activity of recombinant hUCK was evaluated using the nucleoside analogues, N_3-D-dCMP and N_3-D-dUMP (Figure 3). Both compounds were substrates of the enzyme and followed Michaelis–Menten kinetics. High concentrations did not give rise to substrate inhibition of hUCK, unlike the natural substrates, D-CMP and D-UMP. The K_M values were 0.36 mM for N_3-D-dCMP and 0.9 mM for N_3-D-dUMP compared to 20 μM for D-CMP and 50 μM for D-UMP (Table 3). Despite the higher K_M values, the catalytic efficiencies for phosphorylation of the 2′-azido derivatives were in the same order of magnitude (10^5–10^6) as those for the natural substrates of the enzyme. The reaction rate with N_3-D-dUMP was similar to that with D-UMP (Figure 3, Table 3). The reaction rate of hUCK with N_3-D-dCMP was almost 4 times faster than that with D-CMP, demonstrating that N_3-D-dCMP is currently the best-known substrate for hUCK (Figure 3B). Other enzymes hAK1, hAK2 and hTMPK did not significantly phosphorylate these substrates.

The enantioselectivity of hUCK for 2′-azido-2′-deoxynucleoside monophosphates was also evaluated. The K_M value for N_3-L-dCMP was increased (1.2 mM) while the V_{max} was lower ($1.1\,U{\cdot}mg^{-1}$), leading to a 4000-fold lower catalytic efficiency than for the D-enantiomer (Table 3). N_3-L-dUMP was also a poor substrate of the enzyme, with a K_M of 1.3 mM and a k_{cat} of $0.34\,s^{-1}$(Table 3). The 2′-azido group was thus only favourable for the D-analogues. Overall, in the L-series, the pyrimidine 2′-deoxyribonucleotides were better substrates than the pyrimidine ribonucleotides and the 2′-azido-2′-deoxyribonucleotides, indicating that 2′-substitutions may cause steric hindrance for L-NMP binding to hUCK.

Table 3. Catalytic parameters for the (d)CMP, (d)UMP enantiomers and their 2′azido analogues with human UMP-CMP kinase

Substrate	K_M (mM)	Relative V_{max} (%)	k_{cat}/K_M ($M^{-1}\,s^{-1}$)
D-CMP	0.020 ± 0.005	100[a]	6.5×10^6 (100[c])
D-dCMP	1.0 ± 0.1	61 ± 4	7×10^4 (1.2)
L-CMP	0.75 ± 0.07	0.054 ± 0.001	100 (0.0015)
L-dCMP	0.73 ± 0.06	0.63 ± 0.02	1000 (0.015)
N_3-D-dCMP	0.36 ± 0.03	408 ± 9	1.5×10^6 (23)
N_3-L-dCMP	1.2 ± 0.1	0.36 ± 0.02	390 (0.006)
D-UMP	0.05 ± 0.01	100	2.8×10^6 (43)
D-dUMP	1.3 ± 0.3	5.1 ± 0.5	6000 (0.1)
L-dUMP	0.70 ± 0.09	0.28 ± 0.02	530 (0.008)
N_3-D-dUMP	0.9 ± 0.2	89 ± 6	1.4×10^5 (2.15)
N_3-L-dUMP	1.3 ± 0.1	0.07 ± 0.02	270 (0.004)
L-3TCMP[b]	0.15 ± 0.02	27	2.8×10^5 (4.3)

[a]The relative V_{max} was obtained by comparing the k_{cat} value of the substrates to that of D-CMP. V_{max} = 100 corresponds to 350 μmol of substrate transformed/min/mg, i.e. to a $k_{cat} = 130\,s^{-1}$ [from (15)].
[b]data from (15) for comparison.
[c]The relative efficiencies were obtained by comparing the k_{cat}/K_M ($M^{-1}\,s^{-1}$) value of the substrates to that of D-CMP.

Structural analysis of the enantioselectivity of human AMP, TMP and UMP-CMP kinases

The NMP kinases all have a highly conserved structure with a central CORE domain that contains an ATP binding loop (P-loop) and two mobile domains: an NMP binding domain and an LID domain, which provide the catalytic residues for the reaction (39). Both the NMP and LID domains are extremely mobile and undergo large 'hinge bending' motions (40). The same conformational changes are believed to occur in all NMP kinases when they switch from their opened to closed conformation upon substrate binding. The X-ray structure of hAK1 complexed with the bisubstrate inhibitor Ap5A was recently solved: it showed the interactions of AMP with the active site in the closed conformation (41). The structure of hTMPK complexed with various ligands has been thoroughly explored (42), but the structure of the free apoenzyme is not known. In contrast, the structure of hUCK is only known in its open conformation (43). Substrate-free hTMPK probably also exists in an opened conformation and substrate-bound hUCK probably adopts a closed conformation as does the homologous enzyme from *Dictyostelium* (44).

L-AMP and L-dTMP were tentatively docked in the closed conformation of hAK1 and hTMPK, and L-dCMP was docked in an enzyme model based on the *Dictyostelium* UCK (44). The docking of L-(d)AMP in hAK1 failed to provide a model (data not shown): this could be due to the rather specific interactions of D-AMP with the protein, which are not mediated by water molecules, thus limiting its capacity to accommodate other substrates. The docking of L-deoxypyrimidine monophosphates in hTMPK and UCK was more successful (Figures 4 and 5). The dTMP and CMP binding sites are represented as four interacting motifs: (i) the LID domain, (ii) the P-loop, (iii) the mobile part of NMP binding domain and (iv) the stable part of NMP binding domain. The binding of L-dTMP differed from that of D-dTMP, especially at the deoxyribose moiety (Figure 4). The H-bonds between the first layer residues and the thymine ring involved several water molecules, providing a 'flexible' NMP binding domain that readily accommodates modified substrates. The thymine ring was stacked onto Phe72 in L-dTMP binding, but it was not optimal, as the base was shifted through 15°. The interaction of the phosphate group with Mg^{2+} ion and Asp15 in the P-loop, via a water molecule, was conserved, as was its interaction with Arg97 from the mobile NMP domain.

Downloaded from https://academic.oup.com/nar/article/35/14/4895/1014948 by Bibliothèque Universitaire de médecine - Nîmes user on 01 June 2022

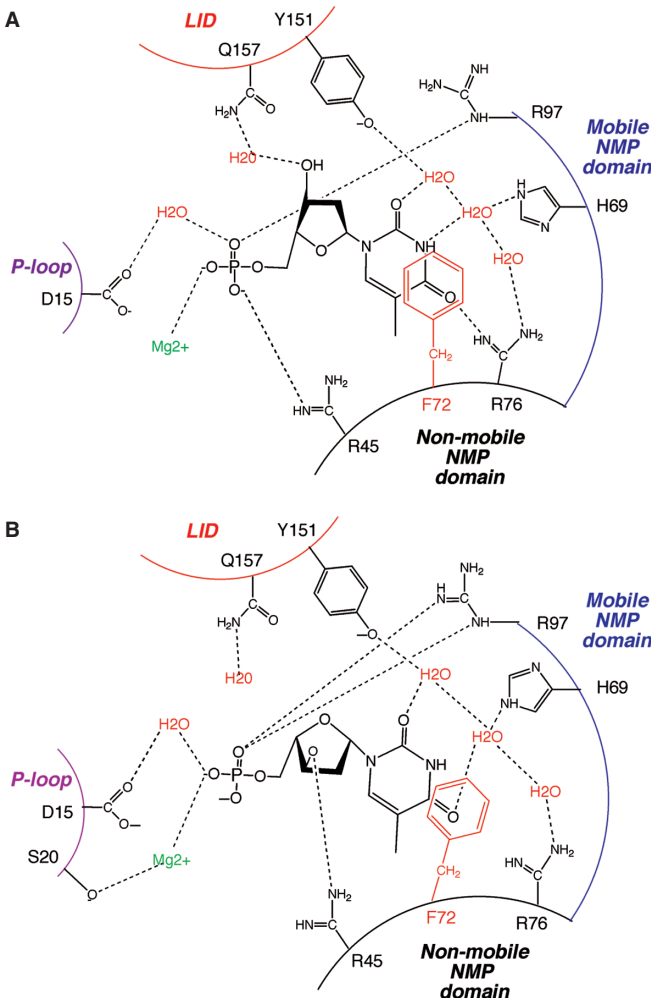

Figure 4. Scheme of the acceptor-binding site of human dTMP kinase in the closed form: (**A**) with D-dTMP bound to the acceptor-binding site; (**B**) with L-dTMP modelled in the acceptor-binding site. LID (red), P-loop (pink), immobile NMP domain (black) and mobile NMP domain (blue).

However, the deoxyribose 3′OH, which interacts with the LID Gln157 via a water molecule in the D-dTMP/hTMPK complex, was modelled as being H-bonded to the NH_2 of the highly conserved Arg45 of the immobile NMP domain in the L-dTMP/hTMPK model.

The major interactions responsible for the binding of D-CMP to hUCK involved the base and phosphate (Figure 5). The interaction of Asn100 with the 4-amino group of the cytidine base played an important role in the base specificity and explains why D-(d)CMP is a better substrate than D-(d)UMP (43). The phosphate does not interact with the P loop as in hTMPK but strongly connects the LID domain (Arg134 and Arg140) to the immobile NMP domain (Arg39, Arg96 and Glu36) (Figure 5A). These residues still interacted with L-dCMP phosphate group in the L-dCMP/UCK model, except for Arg134 (Figure 5B). The cytidine moiety for both D-CMP and L-dCMP was H-bonded to Val63 and Asn100 from the mobile NMP domain, resulting in similar positioning

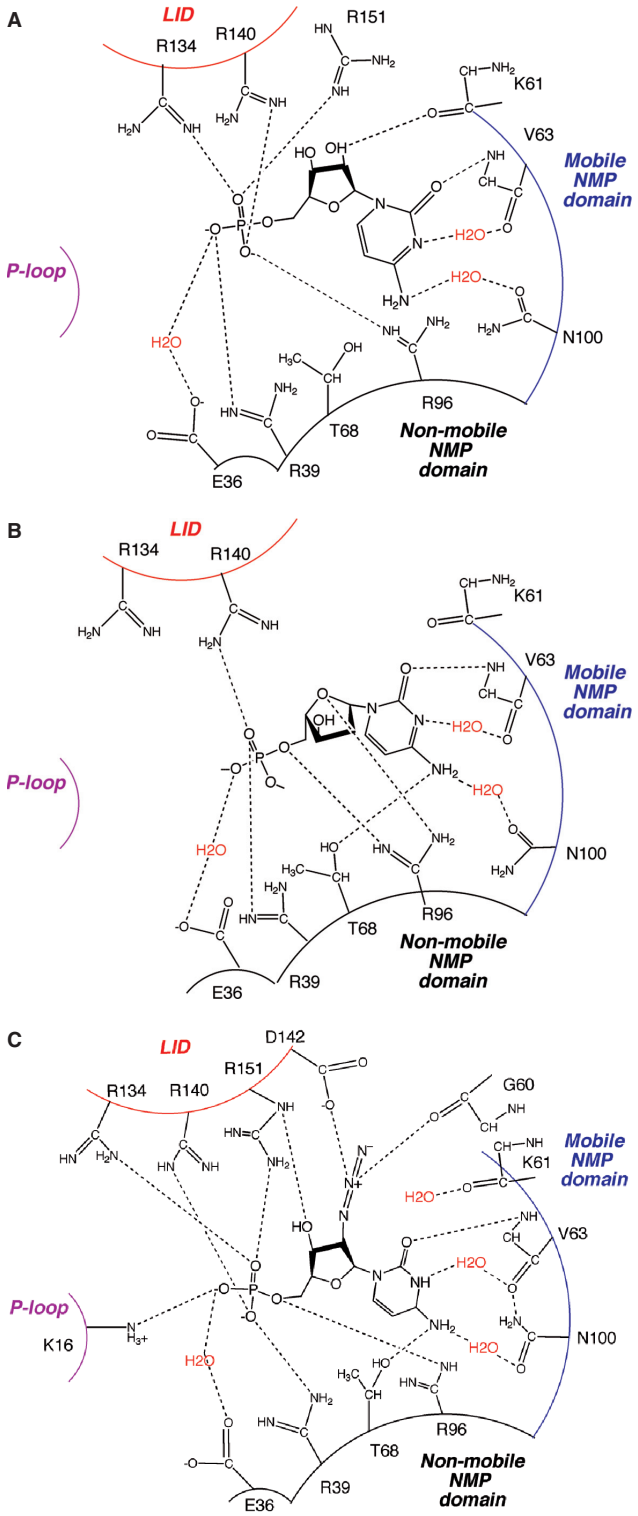

Figure 5. Scheme of the acceptor-binding site of human UMP-CMP kinase in the closed form. (**A**) with D-CMP bound to the acceptor-binding site. (**B**) with L-dCMP modelled in acceptor-binding site. (**C**) N_3-D-dCMP bound to acceptor-binding site.

of the base for both enantiomers. The L-nucleotide did not have the major interaction of the D-CMP 2′OH with the main chain Lys61 carbonyl, contained within the NMP mobile domain. L-dCMP was a better substrate for hUCK

Downloaded from https://academic.oup.com/nar/article/35/14/4895/1014948 by Bibliothèque Universitaire de médecine - Nîmes user on 01 June 2022

than was L-CMP, probably due to 2′-OH steric hindrance. However, the ring oxygen in L-dCMP interacted with Arg96, anchoring the sugar to the immobile NMP domain (Figure 5B).

The model obtained with N_3-D-dCMP bound to hUCK had favourable interactions as the azido group interacts with both Asp142 in the LID domain and the α-carbonyl of Gly60 in the mobile NMP domain (Figure 5C). The 2′OH of the ribonucleotide has been shown to contribute to the LID closure of hUCK by its interaction with the carbonyl of Lys61 located in the mobile NMP domain (43). This interaction also explains the higher affinity of the enzyme for D-ribonucleotides compared to D-deoxyribonucleotides. The replacement of 2′-hydroxyl by a bulkier azido group prevents complete closure of the LID, which results in higher K_M values. However, the opening of the LID, which promotes product release, is proposed to be the rate-limiting step of the reaction catalyzed by hUCK. A recent NMR experiment on hyperthermophilic and mesophilic homologues of AK also suggested that the opening of the AMP binding and/or LID domains upon product release was the rate-limiting step influencing the catalytic turnover (45,46). The azido group might thus facilitate the LID opening or could connect the LID and mobile-NMP domains and synchronize their opening, explaining the higher rate of phosphorylation of N_3-D-dCMP compared to D-CMP. Dynamic studies should help to understand these higher rates.

CONCLUSION

We have compared the activities of the kinases on L- and D-nucleotides and shown that both hTMPK and hUCK have relaxed enantioselectivities for dNMP, while hAK 1 and 2 are strictly devoted to D-(d)NMP. The pyrimidine kinases phosphorylated only L-derivatives of the deoxy series. UCK was active with L-dCMP but far less efficiently than with L-3TCMP (15). hTMPK, hUCK, hAK1 and hAK2 all phosphorylated their respective D-(d)NMP with some minor cross-reactivity. For example, D-CMP was phosphorylated efficiently by hUCK ($k_{cat}/K_M = 6.5 \times 10^6\,M^{-1}\,s^{-1}$) and more slowly by hAK1 and hAK2 (k_{cat}/K_M about $10^4\,M^{-1}\,s^{-1}$). D-dUMP was a better substrate for hTMPK ($k_{cat}/K_M = 2.8 \times 10^4\,M^{-1}\,s^{-1}$) than for hUCK ($k_{cat}/K_M = 6 \times 10^3\,M^{-1}\,s^{-1}$). N_3-D-dCMP was the best D-series substrate for hUCK with a k_{cat} 4-fold higher than that for the natural substrate (D-CMP). This could be due to a tighter interaction between the LID domain and the NMP domain as explained by the structural analysis.

RNAi studies have shown that hTMPK is implicated in the activation of L-FMAU (47). There was generally a good correlation between kinetic studies and the antiviral effect, emphasizing the need for efficient cellular activation of the antiviral drug to its triphosphate form, as shown for L-3TC (15). The present study demonstrates the activity of hTMPK on L-dTMP, even if the catalytic efficiency was relatively low ($k_{cat}/K_M = 900\,M^{-1}\,s^{-1}$). L-dTMP had the highest relative phosphorylation efficiency of all the L-(d)NMP tested. The phosphorylation of L-dTMP correlates with studies on the intracellular metabolism of L-dT in HepG2 cells and primary cultures of human hepatocytes. The conversion of L-dTMP to L-dTDP clearly appears to be the rate-limiting step in both cell types (48). The first phosphorylation of L-dT is believed to be carried out by either hdCK or hTK2 with catalytic efficiencies of $1.6 \times 10^4\,M^{-1}\,s^{-1}$ and $1 \times 10^7\,M^{-1}\,s^{-1}$, respectively (9). The recent crystallization of dCK with L-3TC and troxacitabine shows how the nucleoside binding site of dCK can conserve all essential interactions with these analogues or L-dC and thus maintain productive substrate positioning for phosphoryl-transfer (49). Given the great similarity between dCK and hTK2, we can assume that they are similarly flexible for the productive positioning of L-dT, explaining the high catalytic efficiency. The binding of L-dTMP to hTMPK is not optimal and may be the rate-limiting step in the pathway. NDPK does not recognize L-(d)NDP as substrates and phosphoglycerate kinase is probably involved in the conversion of L-dTDP into L-dTTP, with a catalytic efficiency of $500\,M^{-1}\,s^{-1}$ (18). From these *in vitro* data, the second and third phosphorylation steps have low catalytic efficiencies and appear rate-limiting in the activation pathway. This study demonstrated the relaxed enantioselectivity of hTMPK, which is most likely essential to the formation of L-dTTP *in vivo* and thus to the antiviral properties of L-dT.

ACKNOWLEDGEMENTS

These studies were supported by Université Pierre-et-Marie-Curie-Paris 6 and the French Centre National de Recherche Scientifique (FRE 2852 and ANR-05-BLAN-0368-02) and also by the Association pour la Recherche contre le Cancer. We thank Dr Gilles Gosselin and Idenix Pharmaceuticals for providing L-deoxynucleosides. We also thank Prof. Michèle Reboud (FRE 2852 CNRS-Université Paris 6) for laboratory facilities and Dr Laurent Chaloin (Montpellier) for helpful discussions. We are grateful to Laurence Dugué (Institut Pasteur) for synthesizing MABA-dTDP. The English text was edited by Owen Parkes. Funding to pay the Open Access publication charges for this article was provided by the French Centre de Recherche Scientifique (ANT-05-0368-02).

Conflict of Interest Statement. None declared.

REFERENCES

1. Nair,V. and Jahnke,T.S. (1995) Antiviral activities of isometric dideoxynucleosides of D- and L-related stereochemistry. *Antimicrob. Agents Chemother.*, **39**, 1017–1029.
2. Zemlicka,J. (2000) Enantioselectivity of the antiviral effects of nucleoside analogues. *Pharmacol. Ther.*, **85**, 251–266.
3. Cheng,Y.C. (2001) Potential use of antiviral L(-)nucleoside analogues for the prevention or treatment of viral associated cancers. *Cancer Lett.*, **162**(Suppl.), S33–S37.
4. Mathe,C. and Gosselin,G. (2006) L-Nucleoside enantiomers as antivirals drugs: a mini-review. *Antiviral Res.*, **71**, 276–281.
5. Jurovcik,M. and Holy,A. (1976) Metabolism of pyrimidine L-nucleosides. *Nucleic Acids Res.*, **3**, 2143–2154.

Downloaded from https://academic.oup.com/nar/article/35/14/4895/1014948 by Bibliothèque Universitaire de médecine - Nîmes user on 01 June 2022

6. Bryant,M.L., Bridges,E.G., Placidi,L., Faraj,A., Loi,A.G., Pierra,C., Dukhan,D., Gosselin,G., Imbach,J.L. *et al.* (2001) Antiviral L-nucleosides specific for hepatitis B virus infection. *Antimicrob. Agents Chemother.*, **45**, 229–235.
7. Maury,G. (2000) The enantioselectivity of enzymes involved in current antiviral therapy using nucleoside analogues: a new strategy? *Antivir. Chem. Chemother.*, **11**, 165–189.
8. Munch-Petersen,B., Cloos,L., Tyrsted,G. and Eriksson,S. (1991) Diverging substrate specificity of pure human thymidine kinases 1 and 2 against antiviral dideoxynucleosides. *J. Biol. Chem.*, **266**, 9032–9038.
9. Wang,J., Choudhury,D., Chattopadhyaya,J. and Eriksson,S. (1999) Stereoisomeric selectivity of human deoxyribonucleoside kinases. *Biochemistry*, **38**, 16993–16999.
10. Verri,A., Priori,G., Spadari,S., Tondelli,L. and Focher,F. (1997) Relaxed enantioselectivity of human mitochondrial thymidine kinase and chemotherapeutic uses of L-nucleoside analogues. *Biochem. J.*, **328**(Pt 1), 317–320.
11. Shafiee,M., Griffon,J.F., Gosselin,G., Cambi,A., Vincenzetti,S., Vita,A., Eriksson,S., Imbach,J.L. and Maury,G. (1998) A comparison of the enantioselectivities of human deoxycytidine kinase and human cytidine deaminase. *Biochem. Pharmacol.*, **56**, 1237–1242.
12. Van Rompay,A.R., Johansson,M. and Karlsson,A. (2003) Substrate specificity and phosphorylation of antiviral and anticancer nucleoside analogues by human deoxyribonucleoside kinases and ribonucleoside kinases. *Pharmacol. Ther.*, **100**, 119–139.
13. Yan,H. and Tsai,M.D. (1999) Nucleoside monophosphate kinases: structure, mechanism, and substrate specificity. *Adv. Enzymol. Relat. Areas Mol. Biol.*, **73**, 103–134.
14. Liou,J.Y., Dutschman,G.E., Lam,W., Jiang,Z. and Cheng,Y.C. (2002) Characterization of human UMP/CMP kinase and its phosphorylation of D- and L-form deoxycytidine analogue monophosphates. *Cancer Res.*, **62**, 1624–1631.
15. Pasti,C., Gallois-Montbrun,S., Munier-Lehmann,H., Veron,M., Gilles,A.M. and Deville-Bonne,D. (2003) Reaction of human UMP-CMP kinase with natural and analog substrates. *Eur. J. Biochem.*, **270**, 1784–1790.
16. Kreimeyer,A., Schneider,B., Sarfati,R., Faraj,A., Sommadossi,J.P., Veron,M. and Deville-Bonne,D. (2001) NDP kinase reactivity towards 3TC nucleotides. *Antiviral Res.*, **50**, 147–156.
17. Krishnan,P., Liou,J.Y. and Cheng,Y.C. (2002) Phosphorylation of pyrimidine L-deoxynucleoside analog diphosphates. Kinetics of phosphorylation and dephosphorylation of nucleoside analog diphosphates and triphosphates by 3-phosphoglycerate kinase. *J. Biol. Chem.*, **277**, 31593–31600.
18. Gallois-Montbrun,S., Faraj,A., Seclaman,E., Sommadossi,J.P., Deville-Bonne,D. and Veron,M. (2004) Broad specificity of human phosphoglycerate kinase for antiviral nucleoside analogs. *Biochem. Pharmacol.*, **68**, 1749–1756.
19. Cihlar,T. and Chen,M.S. (1996) Identification of enzymes catalyzing two-step phosphorylation of cidofovir and the effect of cytomegalovirus infection on their activities in host cells. *Mol. Pharmacol.*, **50**, 1502–1510.
20. Feng,J.Y. and Anderson,K.S. (1999) Mechanistic studies comparing the incorporation of (+) and (−) isomers of 3TCTP by HIV-1 reverse transcriptase. *Biochemistry*, **38**, 55–63.
21. Feng,J.Y., Murakami,E., Zorca,S.M., Johnson,A.A., Johnson,K.A., Schinazi,R.F., Furman,P.A. and Anderson,K.S. (2004) Relationship between antiviral activity and host toxicity: comparison of the incorporation efficiencies of 2′,3′-dideoxy-5-fluoro-3′-thiacytidine-triphosphate analogs by human immunodeficiency virus type 1 reverse transcriptase and human mitochondrial DNA polymerase. *Antimicrob. Agents Chemother.*, **48**, 1300–1306.
22. Liou,J.Y., Krishnan,P., Hsieh,C.C., Dutschman,G.E. and Cheng,Y.C. (2003) Assessment of the effect of phosphorylated metabolites of anti-human immunodeficiency virus and anti-hepatitis B virus pyrimidine analogs on the behavior of human deoxycytidylate deaminase. *Mol. Pharmacol.*, **63**, 105–110.
23. Mazzon,C., Rampazzo,C., Scaini,M.C., Gallinaro,L., Karlsson,A., Meier,C., Balzarini,J., Reichard,P. and Bianchi,V. (2003) Cytosolic and mitochondrial deoxyribonucleotidases: activity with substrate analogs, inhibitors and implications for therapy. *Biochem. Pharmacol.*, **66**, 471–479.
24. Thelander,L. and Larsson,B. (1976) Active site of ribonucleoside diphosphate reductase from Escherichia coli. Inactivation of the enzyme by 2′-substituted ribonucleoside diphosphates. *J. Biol. Chem.*, **251**, 1398–1405.
25. Salowe,S., Bollinger,J.M.Jr, Ator,M., Stubbe,J., McCraken,J., Peisach,J., Samano,M.C. and Robins,M.J. (1993) Alternative model for mechanism-based inhibition of Escherichia coli ribonucleotide reductase by 2′-azido-2′-deoxyuridine 5′-diphosphate. *Biochemistry*, **32**, 12749–12760.
26. Roy,B., Verri,A., Lossani,A., Spadari,S., Focher,F., Aubertin,A.M., Gosselin,G., Mathe,C. and Perigaud,C. (2004) Enantioselectivity of ribonucleotide reductase: a first study using stereoisomers of pyrimidine 2′-azido-2′-deoxynucleosides. *Biochem. Pharmacol.*, **68**, 711–718.
27. He,J., Roy,B., Perigaud,C., Kashlan,O.B. and Cooperman,B.S. (2005) The enantioselectivities of the active and allosteric sites of mammalian ribonucleotide reductase. *FEBS J.*, **272**, 1236–1242.
28. Topalis,D., Collinet,B., Gasse,C., Dugue,L., Balzarini,J., Pochet,S. and Deville-Bonne,D. (2005) Substrate specificity of vaccinia virus thymidylate kinase. *FEBS J.*, **272**, 6254–6265.
29. Yoshikawa,M., Kato,T. and Takenishi,T. (1967) A novel method for phosphorylation of nucleosides to 5′-nucleotides. *Tetrahedron Lett.*, **50**, 5065–5068.
30. Xing,J., Apedo,A., Tymiak,A. and Zhao,N. (2004) Liquid chromatographic analysis of nucleosides and their mono-, di- and triphosphates using porous graphitic carbon stationary phase coupled with electrospray mass spectrometry. *Rapid Commun. Mass Spectrom.*, **18**, 1599–1606.
31. Pochet,S., Dugue,L., Labesse,G., Delepierre,M. and Munier-Lehmann,H. (2003) Comparative study of purine and pyrimidine nucleoside analogues acting on the thymidylate kinases of Mycobacterium tuberculosis and of humans. *Chembiochem*, **4**, 742–747.
32. Blondin,C., Serina,L., Wiesmuller,L., Gilles,A.M. and Barzu,O. (1994) Improved spectrophotometric assay of nucleoside monophosphate kinase activity using the pyruvate kinase/lactate dehydrogenase coupling system. *Anal. Biochem.*, **220**, 219–221.
33. Chen,Y., Gallois-Montbrun,S., Schneider,B., Veron,M., Morera,S., Deville-Bonne,D. and Janin,J. (2003) Nucleotide binding to nucleoside diphosphate kinases: X-ray structure of human NDPK-A in complex with ADP and comparison to protein kinases. *J. Mol. Biol.*, **332**, 915–926.
34. DeLano,W. (2002) *The PyMOL Molecular Graphics System.* DeLano Scientific, Palo Alto, CA, USA.
35. Thompson,M. (2004) ArgusLab edn. Planaria Software LLC, Seattle, WA.
36. Noma,T., Fujisawa,K., Yamashiro,Y., Shinohara,M., Nakazawa,A., Gondo,T., Ishihara,T. and Yoshinobu,K. (2001) Structure and expression of human mitochondrial adenylate kinase targeted to the mitochondrial matrix. *Biochem. J.*, **358**, 225–232.
37. Ren,H., Wang,L., Bennett,M., Liang,Y., Zheng,X., Lu,F., Li,L., Nan,J, Luo,M. *et al.* (2005) The crystal structure of human adenylate kinase 6: an adenylate kinase localized to the cell nucleus. *Proc. Natl Acad. Sci. USA*, **102**, 303–308.
38. Arima,T., Akiyoshi,H. and Fujii,S. (1977) Characterization of pyrimidine nucleoside monophosphokinase in normal and malignant tissues. *Cancer Res.*, **37**, 1593–1597.
39. Schulz,G.E., Schiltz,E., Tomaselli,A.G., Frank,R., Brune,M., Wittinghofer,A. and Schirmer,R.H. (1986) Structural relationships in the adenylate kinase family. *FEBS J.*, **161**, 127–132.
40. Vonrheim,C., Schlauderer,G.J. and Schulz,G.E. (1995) Movie of the structural changes during a catalytic cycle of nucleoside monophosphate kinases. *Structure*, **3**, 483–490.
41. Filippakopoulos,P., Bunkoczi,G., Jansson,A., Schreurs,A., Knapp,S., Edwards,A., Von Delft,F. and Sundstrom,M. (2005) Crystal structure of human AK1A in complex with AP5A. *Structural Genomics Consortium Oxford*, PDB code 1Z83.
42. Ostermann,N., Segura-Pena,D., Meier,C., Veit,T., Monnerjahn,C., Konrad,M. and Lavie,A. (2003) Structures of human thymidylate kinase in complex with prodrugs: implications for the structure-based design of novel compounds. *Biochemistry*, **42**, 2568–2577.

Downloaded from https://academic.oup.com/nar/article/35/14/4895/1014948 by Bibliothèque Universitaire de médecine - Nîmes user on 01 June 2022

43. Segura-Pena,D., Sekulic,N., Ort,S., Konrad,M. and Lavie,A. (2004) Substrate-induced conformational changes in human UMP/CMP kinase. *J. Biol. Chem.*, **279**, 33882–33889.
44. Scheffzek,K., Kliche,W., Wiesmuller,L. and Reinstein,J. (1996) Crystal structure of the complex of UMP/CMP kinase from Dictyostelium discoideum and the bisubstrate inhibitor P1-(5′-adenosyl) P5-(5′-uridyl) pentaphosphate (UP5A) and Mg2+ at 2.2 A: implications for water-mediated specificity. *Biochemistry*, **35**, 9716–9727.
45. Wolf-Watz,M., Thai,V., Henzler-Wildman,K., Hadjipavlou,G., Eisenmesser,E.Z. and Kern,D. (2004) Linkage between dynamics and catalysis in a thermophilic-mesophilic enzyme pair. *Nat. Struct. Mol. Biol.*, **11**, 945–949.
46. Bae,E. and Phillips,G.N.Jr (2006) Roles of static and dynamic domains in stability and catalysis of adenylate kinase. *Proc. Natl. Acad. Sci. USA*, **103**, 2132–2137.
47. Hu,R., Li,L., Degreve,B., Dutschman,G.E., Lam,W. and Cheng,Y.C. (2005) Behavior of thymidylate kinase toward monophosphate metabolites and its role in the metabolism of 1-(2′-deoxy-2′-fluoro-beta-L-arabinofuranosyl)-5-methyluracil (Clevudine) and 2′,3′-didehydro-2′,3′-dideoxythymidine in cells. *Antimicrob. Agents Chemother.*, **49**, 2044–2049.
48. Hernandez-Santiago,B., Placidi,L., Cretton-Scott,E., Faraj,A., Bridges,E.G., Bryant,M.L., Rodriguez-Orengo,J., Imbach,J.L., Gosselin,G. *et al.* (2002) Pharmacology of beta-L-thymidine and beta-L-2′-deoxycytidine in HepG2 cells and primary human hepatocytes: relevance to chemotherapeutic efficacy against hepatitis B virus. *Antimicrob. Agents Chemother.*, **46**, 1728–1733.
49. Sabini,E., Hazra,S., Konrad,M., Burley,S.K. and Lavie,A. (2007) Structural basis for activation of the therapeutic L-nucleoside analogs 3TC and troxacitabine by human deoxycytidine kinase. *Nucleic Acids Res.*, **35**, 186–192.

Downloaded from https://academic.oup.com/nar/article/35/14/4895/1014948 by Bibliothèque Universitaire de médecine - Nîmes user on 01 June 2022